Comparison of Zeroth-Order Deterministic Local and Delay Pandemic Models

David L. Bartley
Centers for Disease Control and Prevention, Retired
3904 Pocahontas Avenue, Cincinnati, Ohio 45227
bartleydavy@gmail.com

Abstract. Delay differential equations are set up for zeroth-order pandemic models in analogy with traditional SIR and SEIR models by specifying individual times of incubation and infectiousness prior to recovery. Independent linear delay relations in addition to a nonlinear delay differential equation are found for characterizing time-dependent compartmental populations. Asymptotic behavior allows a link between parameters of the delay and traditional models for their comparison. In analogy with transformation of the traditional equations into linear form giving populations and time in parametric form, approximation of the delay equations results in a simple accurate finite recursive solution. Otherwise, straightforward numerical solution is effected in terms of linearized boundary conditions specifying the distribution of instigators as to their initial infection progress—in contrast to traditional models specifying only initial average infectious and exposed populations. Examples contrasting asymptotically-linked traditional and delay models are given.

Key words. pandemic, models, delay, functional, retarded, neutral

Introduction

The Covid-19 epidemic has aroused great interest in pandemic modelling. This paper addresses two types of compartmental deterministic models. Such models compute the evolution of various populational *compartments* following initial infection Considered here are the classic SIR [7] and SEIR Models which address Susceptible, Exposed, Infectious, and Recovered (including deceased) populations. For a summary and details of these models and their many variations, see [8] and references within. Most [2, 6, 7, 8] of these models are expressed in terms of ordinary nonlinear differential equations local in the time.

Less common are models [1, 5, 10, 11, 12] which specify the rates of change in the populations at a given time in terms of populations at an earlier time. Specifically, this paper considers a pandemic model similar to the traditional SEIR Model (including SIR) constructed by specifying the incubation time τ_δ (for example, 5 days) an individual spends prior to becoming infectious and the total time τ_γ (e.g., 20 days) to recovery. The traditional instantaneous differential equations of the SEIR Model are replaced by *delay* or *functional* nonlocal nonlinear differential equations [3] solvable numerically in terms of the prior history of the initially exposed or infectious. Since in reality, both τ_δ and τ_γ may vary widely between individuals, this type of model, together with the instantaneous or local models, must be considered 0-th order approximations.

The plan for this paper is as follows. First, the delay differential equations are presented, together with various simple relationships among the populations. Asymptotic limits are given. Comparison of the instantaneous and delay models is possible by linking the parameters of the two types of models together requiring asymptotic coincidence. The models are also comparable through the finding of an accurate solution to the delay SIR model in analogy to solution of the usual instantaneous model with populations and time in parametric form from now linear equations, obviating addressing the differential equations numerically. Boundary conditions for the delay models are established that permit specifying the initial distribution of the pandemic instigators in terms of their initial disease progress, unlike the instantaneous models. Finally, several numerical comparisons are made.

Equations of Motion

As with the instantaneous SEIR Model, a function new[t] approximates the rate of new infections per unit time by:

$$new[t] = \frac{\beta}{n}\, i[t]s[t], \tag{1}$$

where β is a rate constant, i[t] is the number of infectious individuals at t, s[t] is the number of those susceptible to infection, and n is the total number of individuals. Following exposure, suppose that an incubation time τ_δ is required until an individual becomes infectious and that a further time interval $(\tau_\gamma - \tau_\delta)$ remains until the individual either recovers or dies.

Suppose the pandemic begins at t = 0 with the introduction of a small number of exposed or infectious individuals. By the time t = τ_γ , all the instigators will have recovered (or died), after which the following conditions hold. The s[t] susceptible individuals at time t > τ_γ consist in all present $(n - e[0] - i[0])$ at t = 0_+ minus those who have become infected after t = 0. Therefore,

$$s[t] = (n - e[0] - i[0]) - \frac{\beta}{n}\int_0^{\mathrm{t}} new[t']\, dt'.$$

At time t, the e[t] exposed individuals are all who suffered new exposures between t − τ_δ and t. Therefore,

$$e[t] = \frac{\beta}{n}\int_{t-\tau_\delta}^{t} new[t]]\, dt' .$$

Similarly, the i[t] infectious individuals at t ($> \tau_\gamma$) consist exactly in those who suffered new exposures between t − τ_γ and t – τ_δ. Therefore,

$$i[t] = \frac{\beta}{n}\int_{\mathrm{t}-\tau_\gamma}^{\mathrm{t}-\tau_\delta} new[t']\, dt' .$$

At t > τ_γ, the r[t] recovered or deceased individuals at t are those who suffered new exposures before t − τ_γ plus the $(e[0] + i[0])$ initially exposed or infectious. Therefore,

$$r[t] = (e[0] + i[0]) + \frac{\beta}{n}\int_0^{\mathrm{t}-\tau_\gamma} new[t']\, dt' \ .$$

The above equations imply, of course, that:

$$\mathrm{s[t]} + e[t] + i[t] + r[t] = n\ (constant). \tag{2}$$

Differentiating the above equations with respect to time t results in an equivalent set of non-local non-linear differential equations:

$$s'[t] = -\frac{\beta}{n} new[t] \tag{3}$$

$$e'[t] = \frac{\beta}{n} new[t] - \frac{\beta}{n} new[\mathrm{t} - \tau_\delta] \tag{4}$$

$$i'[t] = \frac{\beta}{n} new[\mathrm{t} - \tau_\delta] - \frac{\beta}{n} new\left[\mathrm{t} - \tau_\gamma\right] \tag{5}$$

$$r'[t] = \frac{\beta}{n} new\left[\mathrm{t} - \tau_\gamma\right] \tag{6}$$

$$[\Longrightarrow \frac{d}{dt}(s[t] + e[t] + i[t] + r[t]) = 0]. \tag{2}$$

The equations are valid for $t > \tau_\gamma$ and depend for solution on the *functions* i[t] and s[t] given over the interval, $0 < t < \tau_\gamma$ as the initial values, unlike the boundary conditions at a *single point* with ordinary differential equations, hence the aptness of the term, *functional* differential equation. As detailed below, the boundary conditions, i[t] and s[t] over this early interval, are determined by the *distribution* in the exposure times of the initially exposed or infected who trigger the pandemic.

The above equations are analogous to the local SEIR Model in widespread use:

$$s'[t] = -\frac{\beta}{n} new[t] \tag{3}$$

$$e'[t] = \frac{\beta}{n} new[t] - \delta\, e[t] \tag{4'}$$

$$i'[t] = \delta\, e[t] - \gamma\, i[t] \tag{5'}$$

$$r'[t] = \gamma\, i[t]. \tag{6'}$$

Relationships

Both the delay and instantaneous models are characterized as above by actually only *three* equations in the three functions s[t], e[t], and i[t]. In fact, there is a simple relation between s and r.

SEIR:

In the case of the instantaneous model, Equations (1 and 4') imply that

$$\frac{ds}{dr} = \frac{-\beta}{n\gamma} s \implies$$

$$s[r] = n\, e^{-\beta r/n\gamma}, \tag{7}$$

which satisfies $s[0] \sim n$ at $r = 0$ (at $t = 0$).

Delay SEIR:

With the less familiar delay model, Equation (7) holds only asymptotically (at $t \to \infty$ or 0). In addition to

$$s[t] + e[t] + i[t] + r[t] = n, \tag{2}$$

there are two independent nonlocal relations among s, e, i, and r. At t > τ_γ, new infections created at t result in new recoveries at t + τ_γ, so the recovery rate must lag behind the creation rate by τ_γ. Explicitly, Equations (3 and 6) imply that

$$s'[t] + r'\left[t + \tau_\gamma\right] = 0 \implies$$

$$s[t] + r\left[t + \tau_\gamma\right] = n,$$

where the integration constant n is determined by the $t \to \infty$ limit. Equations (4 and 5) then imply:

$$e[t] + i[t] = r\left[t + \tau_\gamma\right] - r[t]. \tag{8}$$

Similarly, infectiousness lags infection by τ_δ , and Equations (3 and 4) give:

$$e'[t] = s'[\mathrm{t} - \tau_\delta] - s'[t], \text{and}$$

$$e[t] = s[\mathrm{t} - \tau_\delta] - s[t], \tag{9}$$

as the $t \to \infty$ limit $\Longrightarrow$ the integration constant = 0. As easily seen, the above relations hold for the simpler SIR Models as well (setting e[t] and τ_δ equal to zero). Equations (2, 3, 8, and 9) together with boundary conditions are then sufficient to determine the evolution of the four populations.

Asymptotic limits

SEIR:

Another similarity between the delay and instantaneous model is found in the asymptotic limits ($t \to \infty$) of s[t] and r[t]. As $t \to \infty$, i[t] and e[t] $\longrightarrow$ 0, and so

$$r_\infty + s_\infty = \mathrm{n}.$$

In the familiar case of the local SEIR model [6, 9], Equation (7) implies:

$$r_\infty + n\, e^{-\beta r_\infty / n\gamma} = n. \tag{10}$$

Solutions r_∞[n] of this transcendental equation have been tabulated as the Lambert W function or the ProductLog in *Mathematica.*

Delay SEIR:

The Delay SEIR Model is somewhat more complicated, but results in an expression of the same form as Equation (10). One approach is to expand the various functions in τ_γ and τ_δ. Equation (8) implies:

$$e[t] + i[t] = \tau_\gamma\, r'[t] + O[\tau_\gamma{}^2].$$

Equations (9 and 6) imply:

$$e[t] = -\tau_\delta\, s'[\mathrm{t}] + \mathrm{O}[\tau_\delta{}^2] = \tau_\delta\, r'[\mathrm{t}] + \mathrm{O}[\tau_\delta{}^2] + O[\tau_\delta\, \tau_\gamma].$$

Therefore, keeping only terms linear in τ_δ or τ_γ,

$$i[t] \sim (\tau_\gamma - \tau_\delta)\, r'[t].$$

Equations (1 and 3) then give

$$s'[t] \sim -\frac{\beta}{n}(\tau_\gamma - \tau_\delta)\, r'[t]\, s[t],$$

which integrates to:

$$s[r] = s_0\, e^{-\frac{\beta}{n}(\tau_\gamma - \tau_\delta)\, r + \cdots} \quad ,$$

where s_0 ensures $s[0] = s_0$. Finally, in the limit t → ∞, where i and e → 0,

$$r_\infty + s_0\; e^{-\frac{\beta}{n}(\tau_\gamma - \tau_\delta) r_\infty} \;= n \qquad (10')$$

Again, the asymptotic value r_∞ is given in terms of the Lambert W function.

Asymptotic linking of the models

In the sections below, the delay and instantaneous models are placed on an equal footing for comparison by identifying the infectious-time constant γ^{-1} with $(\tau_\gamma - \tau_\delta)$, the time an individual is infectious, and the exposed-time constant δ^{-1} with τ_δ, i.e., with the means of the corresponding exponential distributions. Also, as indicated by Equations (10 and 10'), the former identification forces the asymptotic limits to be identical.

Partial solutions

SIR: The traditional SIR Model is easily transformed [4] into a set of linear equations by replacing the independent variable t by an alternative variable η via $i[t]dt = d\eta$. Then $i[\eta]$ and $s[\eta]$ can be easily expressed in closed form, and $t[\eta]$ is determined by evaluating the integral $\int i[\eta]^{-1} d\eta$ numerically. The resulting parametric representation of i, s, and t in terms of η replaces numerical solution of the original nonlinear differential equations.

Delay SIR: No similar transform of the Delay SIR Model is known. Appendix A illustrates the complications of such a parametric solution. Also, Appendix B presents a particular solution smoothing over the initial conditions. However, the following approximation results in a partial solution. Equation (8) can be rewritten as:

$$i[t] = s[t - \tau_\gamma] - s[t]. \tag{8'}$$

If the RHS is approximated as 0th order $i_0[t]$ as,

$$i_0[t] = -\tau_\gamma \, s_0'[t - \tau_\gamma/2], \tag{8''}$$

then Equation (3) simplifies to:

$$s_0'[t] = \frac{\beta\tau_\gamma}{n} s_0[t] \, s_o'[t - \tau_\gamma/2]. \tag{3'}$$

Equation (3') is a *neutral* delay differential equation (i.e., with delay in the derivative [3]) which integrates to

$$s_0[t] = c \, e^{\frac{\beta\tau_\gamma}{n} s_0[t - \tau_\gamma/2]} \tag{11a}$$

$$s[t] = s_0[t + \alpha\tau_\gamma], \tag{11b}$$

where the constant c is determined by initial conditions, avoiding discontinuities [3] in the function $s_0[t]$ and its derivatives.

Equation (11a) is a recurrence relation ending after a finite number of iterations from any time $t > \tau_\gamma$ down to within a boundary interval $[\frac{1}{2}\tau_\gamma, \tau_\gamma]$, where the initial $s[t]$ is defined in terms of the pandemic instigators as described below. Equation (11a) is evaluated for $s_0[t]$ automatically in programs such as *Mathematica*.

Numerical experimenting indicates that the global approximation given in (11a) has an O[τ_γ] shift from s[t] near the peak in i[t] and inflection in s[t]. This shift arises from the inaccuracy of the approximation (8''): Correction of Equation (8'') by simply assuming increase in $-s'[t]$ of the order of $e^{\beta t}$shifts the argument of (8'') down from $\tau_\gamma/2$ by about $0.1\tau_\gamma$ for R[0] ($= \beta\tau$, the initial individual infectiousness) between 2 and 3, resulting in a negative shift of the maximum in $i[t]$ between 70% and 80% of τ_γ.

This result suggests the function $s[t]$ (11b), shifting $s_0[t]$ by $\alpha\tau_\gamma$, $\alpha = O[1]$. The infectious population $i[t]$ is then determined directly from Equation (8'). The accuracy of Equation (11b) (away from the boundary conditions near t = 0, yet retaining their causative effect) is illustrated in Fig. 1 by comparison to the exact numerical solution of the original nonlinear equations for two values of the infection rate β, with $\alpha = 1.25$. Aside from β, the assumed conditions are as in Fig. 2 below. The fractional shift α depends weakly on the

specifics of the boundary conditions, but is insensitive to β or τ_γ . The extreme accuracy of this approximation with R[0] between 2 and 3 and with τ_γ at least as large as 30 is as yet not understood.

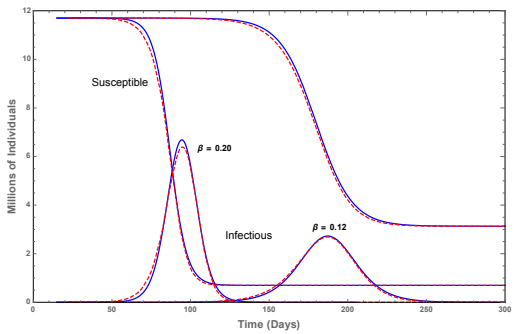

Figure 1. Comparison of approximate recursive (dashed) and exact numerical (solid) solutions of the delay SIR equations at τ_γ =15 days for two different values of the infection rate β.

Linearized Boundary Conditions

Although the above delay differential equations are non-linear, near the start of a pandemic with a small number of infected individuals, a linearized version of the equations is extremely accurate. The corresponding solutions for $t < \tau_\gamma$ are simple and transparent. Furthermore, superposition makes possible the combination of the initially infected as distributed over a range of infection stages. Therefore, the boundary conditions (for time $t < \tau_\gamma$) that reflect the history of the initially infected are easily determined and permit solution of the nonlinear delay equations at $t > \tau_\gamma$ using the same numerical methods as with instantaneous nonlinear equations.

Delay SIR Model:

The earliest times in a pandemic are special in that only the initially infected can recover at $t < \tau_\gamma$, within which explicit solution of s[t] is possible. For example, with the Delayed SIR Model, as long as no recovery occurs by time t,

$$i'[t] = +\frac{\beta}{n} i[t]s[t]$$
$$s'[t] = -\frac{\beta}{n} i[t]s[t].$$

These equations are easily solved in terms of the logistic function, since $i + s + r = n$ (and $r = 0$ and n are constants). However, for the reasons outlined above, at $t < \tau_\gamma$ the linearized equation is adopted:

$$i'[t] = +\frac{\beta}{n} i[t]\, n.$$

Then an initially infectious component i_0 with time t_r remaining prior to recover results in infections $i[t]$ expanding exponentially in time as:

$$i[t] = i_0 e^{\beta t} \quad (t < t_r).$$

Then following recovery of the initial infection at $t = t_r$,

$$i[t] = (i_0 e^{\beta t_r} - i_0) e^{\beta (t - t_r)} \quad (t > t_r).$$

In other words,

$$i[t] = i_0 e^{\beta t}(1 - \theta[t - t_r] e^{-\beta t_r}) \quad (t < \tau_\gamma) \tag{12}$$

$$r[t] = i_0 \theta[t - t_r]$$

$$s[t] = n - i[t] - r[t].$$

Now if there is a distribution $\rho[t_r]$ in the time t_r to recovery of the initially infectious, then superposition implies that the infectious $i[t]$, recovered $r[t]$, and susceptible $s[t]$ at early times are given by

$$\begin{aligned} & t \le \tau_\gamma : \\ & i[t] = e^{\beta t}(i[0] - \textstyle\int_0^t \rho[\, t_r] e^{-\beta t_r} dt_r) \\ & r[t] = \textstyle\int_0^t \rho[\, t_r]\, dt_r \\ & s[t] = n - i[t] - r[t]\,. \end{aligned} \tag{13}$$

These easily-coded functions of t supply the required information for numerical solution of the nonlinear delay differential equations for later time t. The remarkable feature of the delay model is that solutions i[t], r[t], and s[t] depend on an entire initial function, $\rho[t_r]$.

Incidentally, the density $\rho[\tau_i, t]$ at later times ($t > 2\tau_\gamma$) of the infectious vs the length of time τ_i infectious (i.e, $\tau_\gamma - \tau_i = t_r$ is the time to recovery) is given by:

$$\rho[\tau_i, t] = \frac{\beta}{n} i[t - \tau_i\,] s[t - \tau_i\,], \tag{14}$$

which is justified by:

$$\int_0^{\tau_\gamma} \rho[\tau_i, t]\, d\tau_i = -\int_t^{t-\tau_\gamma} \frac{\beta}{n} i[t'] s[t']\, dt' = i[t]. \tag{15}$$

Any "old" case prior to $t - \tau_\gamma$ has "recovered" by the time t; Equation (15) expresses the fact that only the new infections need to be considered for the density at time t. The boundary conditions for the delayed SEIR Model can be expressed similarly to Equations (13), but are somewhat more complicated and are often more simply determined by numerical solution.

Numerical Comparisons

The differences between the delay and local models are best illustrated by means of numerical examples. Parameters for the above models were selected as follows:

$\beta = 0.20\ days^{-1}$
$\tau_\gamma = 20\ days$ for SEIR models
$\tau_\gamma = 15\ days$ for SIR odels
$\tau_\delta = 5\ days$, SEIR
$\tau_\delta = 0\ days$, SIR
$\gamma = (\tau_\gamma - \tau_\delta)^{-1}$
$\delta = {\tau_\delta}^{-1}$
$n = 11.7\ 10^6$

These parameters imply the infectiousicity index R[t] is equal to 3 at t = 0 (i.e., at the start of the pandemic). R[t] is the mean number of infections caused by an individual infectious from time t and can be computed in terms of the susceptible population s[t] as:

$$R[t] = \int_t^{t+\tau_\gamma} \frac{\beta}{n} \mathrm{s[t']\ dt'} \qquad \text{delay SIR}$$
$$R[t] = \int_t^{\infty} e^{-\gamma(t'-t)}\ \frac{\beta}{n} \mathrm{s[t']\ dt'} \qquad \text{local SIR}$$

R[0] and R[∞] are given simply in terms of s[0] and s[∞], in regions of t where s[t] hardly varies.

Illustrating Equations (13), an even initial exposure density $\rho[t_r] = 1/\tau_\gamma$ was selected for the Delay SIR Model and instigating population = 1 for the corresponding Local SIR Model. The integral in Equation (13) then easily provides sufficient information for numerical solution (using Mathematica) for arbitrary time. The results (assuming no mitigation) are illustrated in Figs. 2 and 3.

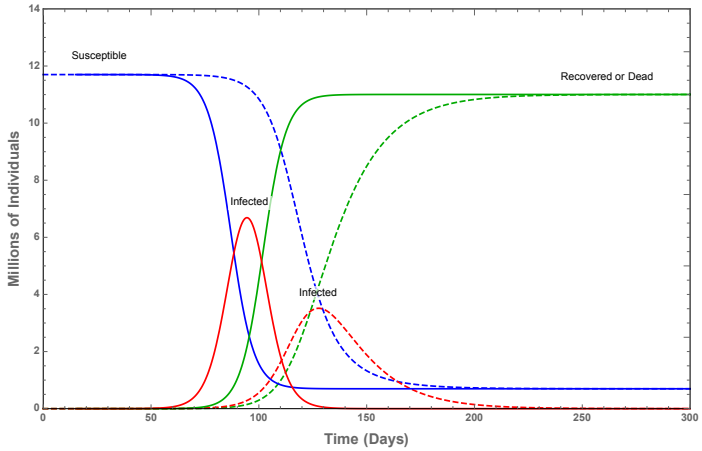

Figure 2. Comparison of the susceptible, infectious, and recovered (or deceased) populations from asymptotically identical SIR models, local (dashed) and delay (solid) with constant distribution of initial exposing factor at infected population = 1 (other parameters in text).

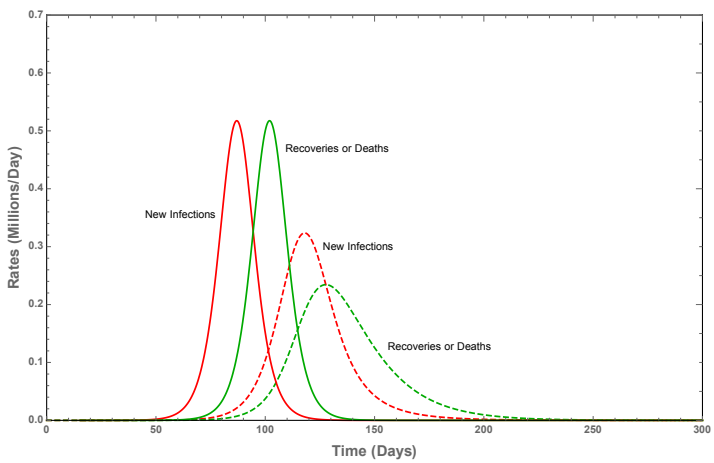

Figure 3. Comparison of the new infections/day and recoveries/day according to local (dashed) and (solid) delay SIR models.

Note the identical asymptotic behavior of the populations in accordance with Equations (10 and 10'). Also, the local curves lag behind those of the delay model, by 1-2 months. The curves for the new cases/day attain maxima at 87 days and 118 days for the delay model and local model, respectively. This lag is not surprising as the probability of continued infectiousness of an individual falls off as e^{-t/τ_γ} for the local model, whereas the probability remains equal to 1 from t = 0 until recovery at t = τ_γ. Also, note the near-symmetry of the curves from the delay model and close relation to the logistic function.

At the opposite extreme from an even density, calculations were also done for sharply peaked densities at a variety of initial recovery times of the instigating individuals. The

results for the SIR models are shown in Fig. 4. The time required for attaining a maximum (as in Fig. 3) in the new cases/day was determined for each initial recovery time. The curve for the delay model is remarkably flat, despite upward turning for the nearly recovered instigator, and, of course, the approach to infinity in the limit of an initially recovered individual. The difference between local and delay models is close to that of the even distribution over the initial recovery times, despite the nonlinearity of the equations.

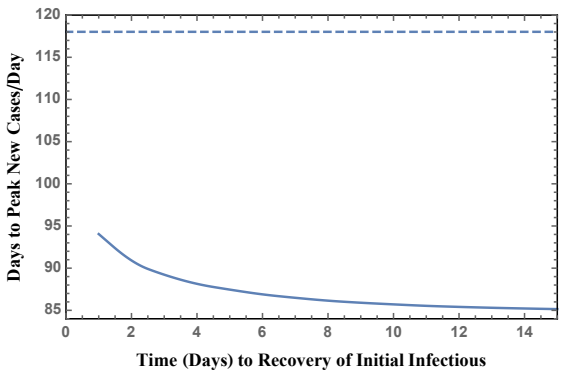

Figure 4. SIR: time to maximum new cases/day in terms of state of health of the initial exposing population = 1 at t = 0.

A similar calculation was done using the SEIR models. A typical result is shown in Fig. 5.

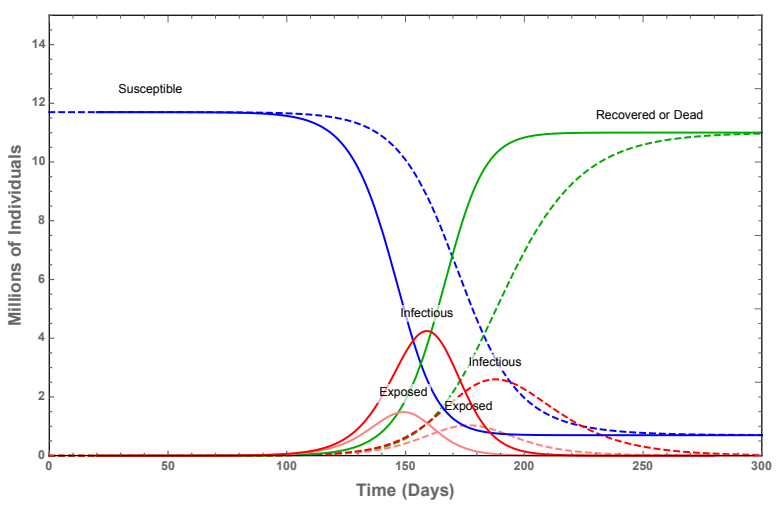

Figure 5. Typical solution for inclusion in the compilation of Figure 6. Local (dashed) and (solid) delay SEIR models.

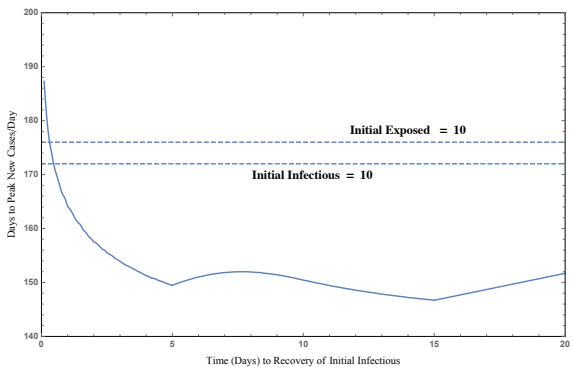

Figure 6. SEIR: time to maximum new cases/day in terms of state of health of the initial exposing population = 10 at t = 0 (other parameters in text). Dashed: local, Solid: delay.

In this case, the linearized boundary conditions were determined numerically. This required attention to the three separate situations: $t_r < \tau_\delta$, $\tau_\delta < t_r < \tau_\gamma - \tau_\delta$, and $\tau_\gamma - \tau_\delta < t_r < \tau_\gamma$ where the initial instigators were only exposed prior to becoming infectious. Again, the increase in the time to maximum in the new cases/day on approaching nearly recovered instigators is apparent, yet is limited to the lowest few days prior to recovery. The difference between local and delay models is similar to that of Fig. 4 for the SIR model, although time from pandemic start to maximum in the new cases/day is naturally longer for the SEIR model with time required for infectiousness to begin.

Conclusions

Similarities and differences are found between basic simple deterministic pandemic models—instantaneous vs delay. Both types of models expressed in terms of differential equations are readily addressed using established techniques of numerical analysis. Interestingly, though nonlinear, both can be expressed in terms of accurate closed-form solutions. Just as the instantaneous equations are very simply linearized in terms of population compartments and time in parametric form, the delay equations admit a simply-evaluated recursive solution. Further research into this solution is merited, for example, explaining the accuracy attained over a wide range of model parameter values.

Both model types share the functional form of asymptotic values relevant to the pandemic winding down. This allows linkage between model types for comparison. Equivalently, parameters can be chosen to equate growth at the pandemic start.

A difference between the models exists in the form of the initial boundary conditions. The delay equations depend on an initial *function*. This function can be expressed in terms of the distribution of pandemic instigators as to initial disease progress. This expression is facilitated by adopting accurate linear boundary conditions permitting superposition even though the equations valid during the progress of the pandemic are nonlinear.

The results of this work show significant difference between the usual local and the delay models *between* the start and death of the pandemic. The difference no doubt relates to the individual's probability of remaining infectious. With the usual local model, this probability falls rapidly as e^{-t/τ_γ} or $e^{-t/(\tau_\gamma-\tau_\delta)}$ where t is the time from the start of infectiousness. In contrast, with the delay model considered here, the probability of infectiousness lasting until time t remains high at 1.00 until the time τ_γ or $\tau_\gamma - \tau_\delta$ is reached.

This difference may be significant to the progress of a pandemic. The ultimate result as the pandemic winds down is identical for the two types of models considered here. Of course, it is the progress up to the time of the maximum in the new cases/day that is necessary to understand in order to adopt appropriate mitigating measures.

These results may provide help in choosing between the models. From the point of view of calculation, the delay model is not significantly more difficult to analyze. Which model is appropriate depends on the details of recovery or death of the individual following infection.

References

[1] M. E. ALEXANDERA, S. M. MOGHADASA, G. RÖSTD, AND J. WU , *A Delay Differential Model for Pandemic Influenza with Antiviral Treatment*, Bulletin of Mathematical Biology 70 (2008), pp. 382–397.

[2] F. BRAUER, *Mathematical epidemiology: Past, present, and future*, Infect. Dis. Model, 2 (2017), pp. 113–127.

[3] J. K. HALE, Functional Differential Equations, Applied Math. Sci., Springer-Verlag, Berlin, 1977.

[4] T. HARKO, F. S. N. LOBO, AND M. K. MAK, *Exact analytical solutions of the Susceptible-Infected-Recovered (SIR) epidemic model and of the SIR model with equal death and birth rate*s, Applied Mathematics and Computation, 236 (2014), pp.184–194.

[5] H. W. HETHCOTE, M. A. LEWIS, AND P. VAN DEN DRIESSCHE, *An epidemiological model with a delay and a nonlinear incidence rate*, Journal of Mathematical Biology, 27 (1988), pp. 49-64.

[6] H. W. HETHCOTE, *The Mathematics of Infectious Diseases,* SIAM Review, 42 (2000), pp. 599–653.

[7] W. O. KERMACK AND A. G. MCKENDRICK, *A Contribution to the Mathematical Theory of Epidemics,* Proceedings of the Royal Society A., 115 (1927), pp. 700–721.

[8] A. MENON, N. K. RAJENDRAN, A. CHANDRACHUD, AND G. SETLUR, *Modelling and simulation of COVID-19 propagation in a large population with specific reference to India,* medRxiv 2020.04.30.20086306

[9] J. C. MILLER, *A note on the derivation of epidemic final sizes*, Bulletin of Mathematical Biology, 74 (2012).

[10] Y. NAKATA, T. OMORI, *Delay equation formulation for an epidemic model with waning immunity: an application to mycoplasma pneumoniae*, IFAC PapersOnLine, 48 (2015), pp. 132-135.

[11] J. SWITKES, *A modified discrete SIR model*, College Math. J., 34 (2003), pp. 399–402.

[12] R. XU AND Z. MA, *Stability of a delayed sirs epidemic model with a nonlinear incidence rate*, Chaos, Soliton and Fractals, 41 (2009), pp. 2319–2325.

Appendix A -- Parametric Approximation to the Delay SIR Model

The identical change of independent variable via $i[t]dt = d\eta$ linearizing the SIR Model can be applied to the Delay SIR and leads to an approximation analogous to Equation (8''). The subsequent calculation is not as comfortable practically as that given by Equation (11), and the solution is not as accurate as that depicted in Fig. 1. Nevertheless, the result, though somewhat negative, merits reporting and does have interesting aspects.

As with the SIR Model, $\mathrm{t}[\eta]$ is given by:

$$\mathrm{t}[\eta] = \tau_\gamma + \int_0^\eta d\eta'/i[\eta'] \tag{A1}$$

if $\eta = 0$ is identified with $\mathrm{t} = \tau$. Also, like SIR, Equation (3) becomes linear:

$$ds/d\eta = -\frac{\beta}{n}s,$$

which integrates to:

$$s[\eta] = s[\tau_\gamma]e^{-\frac{\beta}{n}\eta}, \tag{A2}$$

where the constant $s[\tau_\gamma]$ is the value of the susceptible population at $\mathrm{t} = \tau_\gamma$.

The difficult part is handling Equation (8'):

$$i[t] = s\left[t - \tau_\gamma\right] - s[t]. \tag{8'}$$

Expressed in terms of η via Equation (A1),

$$i[\eta + \delta\eta] = s[\eta] - s[\eta + \delta\eta], \tag{A3}$$

meaning that:

$$i[\int_0^{\eta+\delta\eta}] = s[\int_0^{\eta}] - s[\int_0^{\eta+\delta\eta}].$$

With t in (8') given by

$$t = \left(t - \tau_\gamma\right) + \tau_\gamma$$

$$= \int_0^{\eta+\delta\eta},$$

$$\tau_\gamma = \int_\eta^{\eta+\delta\eta} d\eta'/i[\eta']. \tag{A4}$$

Here is where an approximation can be taken. Suppose the RHS of (A4) is approximated via trapezoidal integration by:

$$\tau_\gamma = \tfrac{1}{2}\delta\eta\left[\frac{1}{i[\eta]} + \frac{1}{i[\eta+\delta\eta]}\right]. \tag{A5}$$

Equations (A2 and A3) then imply:

$$i[\eta + \delta\eta] = s[\tau_\gamma]e^{-\frac{\beta}{n}\eta}[1 + e^{-\frac{\beta}{n}\delta\eta}], \tag{A6}$$

with $\delta\eta$ given by (A5).

$i[\eta]$ is easily expressed in terms of $i[\eta + \delta\eta]$. However, recursion from η back to the boundary interval is not possible because $\delta\eta$ depends on η. Instead, a *forward* recursion *from* the boundary interval, where $i[\eta]$ is specified, may be taken.

Solving for $i[\eta + \delta\eta]$ is not comfortable, but one approach is to select a representative point t_0 (more accurately, a *set* of initial points) in the boundary $[0, \tau_\gamma]$ where $i[t]$ is given. Then the corresponding η_0 and $i[\eta_0]$ are determined, whereupon (A5 and A6) are solved for $i[\eta_0 + \delta\eta]$ and $\delta\eta$ by usual numerical means. This is repeated a number (e.g., 20) times, giving a sequence of values $i[\eta_1]$, $i[\eta_2]$, … . Finally, the function $i[\eta]$ is represented by interpolation.

This procedure, combining results from $t_0 = (0.00, 0.25, 0.50, 0.75, \text{and } 1.00)*\tau_\gamma$, was done for the conditions at $\beta = 0.20$ and $\tau_\gamma = 15$ days as in Fig. 1. The time t[η] in parametric form was then computed from Equation (A1) and is shown in Fig. A1.

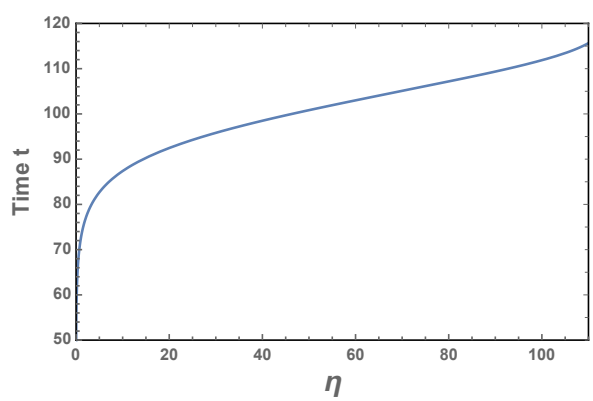

Figure A1. The time t in terms of parameter η.

The three functions $s[\eta]$, $i[\eta]$, and $t[\eta]$ in parametric form then give the susceptible and infectious populations vs time t (shifted by τ_γ as in 11') as seen in Fig. A2.

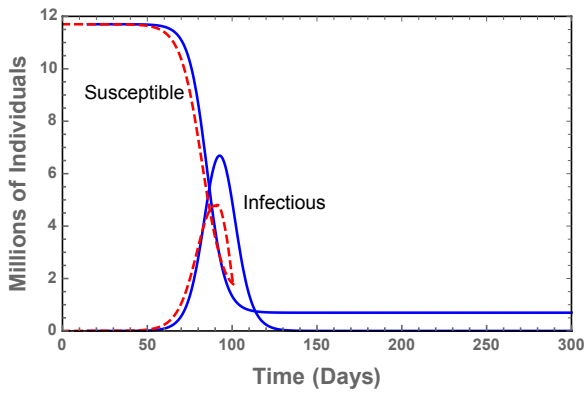

Figure A2. Exact (solid) and parameterized (dashed) populations vs time.

Comparing Figs. (1 and A2) the parametric approximation is inferior to the simple recursive solution (11) behind Fig.1. One interesting feature is that Fig. A2 requires a shift by $[O[\tau_\gamma]$ as in (11'), evidently a feature of the inaccuracy of the trapezoidal integration (A5). Another aspect worth exploring is the degree to which the boundary details survive to the time of the maximum in $i[t]$. These details are no doubt present in any interval larger than τ_γ, but some appear so dominated at large t by an "asymptotic" function as to be invisible on the scale of Fig. A2. This would indicate that only a limited set of representative initial points t_0 may be required to observe the main features of the populations.

Appendix B – Particular Soliton Solution to the Delay SIR Model

Numerical experimenting indicates that varying the boundary conditions at the start of a pandemic, holding β and τ constant, simply shifts the compartment curves in time (at the scale of the figures in this paper). This suggests a soliton-like solution extending from t = $-\infty$ to $+\infty$. Furthermore, the symmetry and shape of the curves depicting the infectious population and the new-infection rate suggest a logistic rather than gaussian model, at least in approximation.

Therefore, the susceptible population may be taken as:

$$sSol[t] = s_{-\infty} + \frac{s_{+\infty} - s_{-\infty}}{1 + e^{-b(t-t_i)}}, \tag{B1}$$

where $s_{+\infty}$ represents the asymptotic value, $s_{-\infty}$ is a value at time t near 0, approximately the initial susceptible population or the total population n, and t_i is the time of inflection in the susceptible population. The parameter b is to be determined to best solve Equations (3 and 8'):

$$s'[t] = -\frac{\beta}{n} s[t](s[t - \tau_\gamma] - s[t]). \tag{B2}$$

Substituting sSol[t] for s[t], results in an exact solution of Equation (B2), iff

$$\frac{s_{-\infty}}{s_{+\infty}} = e^{\beta\tau_\gamma}, \text{ and}$$

$$b = -\frac{\beta}{n} s_{+\infty} (1 - e^{\beta\tau_\gamma})$$

$$= -\frac{\beta}{n} (s_{+\infty} - s_{-\infty}).$$

Then if $s_{-\infty}$ is approximated as n,

$$b = \frac{\beta}{n} r_\infty, \text{ and}$$

$$\text{n } e^{-\frac{\beta}{n} r_\infty \tau_\gamma} \sim n - r_\infty, \tag{B3}$$

a close approximation to the asymptotic result in Equation (10').

The accuracy of Equations (B1 and B3) is illustrated in Fig. B1.

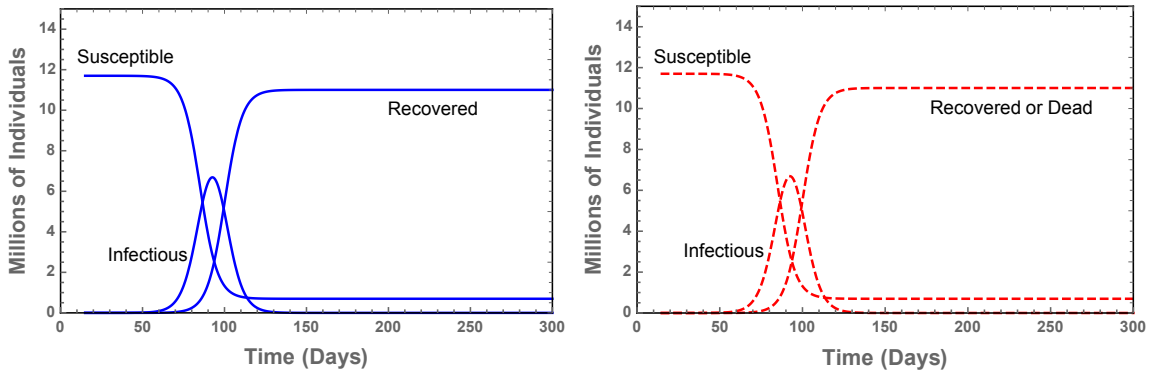

Figure B1. Comparison of exact numerical solution (solid) to the soliton approximation (dashed) with parameters similar to Fig. 1.

The curve shapes are indistinguishable. Of course, the inflection time t_i was taken from the numerical result. Changing boundary conditions simply shifts the curves in time leaving their shapes invariant as with the approximation in Equation (11). Also, the soliton solution cannot reproduce the fine details in the curves near $t = 0$ where the boundary function is important.